Scalar Meson σ Phase Motion at $D^+ \to \pi^-\pi^+\pi^+$ Decay

Ignacio Bediaga
Centro Brasileiro de Pesquisas Físicas-CBPF
Rua Xavier Sigaud 150, 22290-180 Rio de Janeiro, Brazil
(Representing the Fermilab E791 collaboration.)

Received on 14 January, 2004

We make a direct and model-independent measurement of the low $\pi^+\pi^-$ mass phase motion in the $D^+ \to \pi^-\pi^+\pi^+$ decay. Our preliminary results show a strong phase variation, compatible with the isoscalar $\sigma(500)$ meson. This result confirms our previous result [1] where we found evidence for the existence of this scalar particle using full Dalitz-plot analysis. We apply the Amplitude Difference (AD) method [2] to the same Fermilab E791 data sample used in the preceding analysis. We also give an example of how we extract the phase motion of the scalar amplitude, looking at the $f_0(980)$ in $D_s^+ \to \pi^-\pi^+\pi^+$ decay.

1 Introduction

Fermilab experiment E791, with a full Dalitz plot analysis, showed strong evidence for the existence of light and broad scalar resonances in charm D^+ meson decay [1, 3]. The $\pi^+\pi^-$ resonance is compatible with the isoscalar meson $\sigma(500)$, and was observed in the Cabbibo-suppressed decay $D^+ \to \pi^-\pi^+\pi^+$. To get a good fit quality in this analysis, it was necessary to include an extra scalar particle, other than the well established dipion resonances [4]. For the new state, modeled by a Breit-Wigner amplitude, it was measured a mass and width of $478^{+24}_{-23} \pm 17$ MeV/c^2 and $324^{+42}_{-40} \pm 21$ MeV/c^2respectively . The $D^+ \to \sigma(500)\pi^+$ decay contribution is dominant, accounting for approximately half of this particular $D^+ \to \pi^-\pi^+\pi^+$ decay. We found also evidence for a scalar $K^-\pi^+$ resonance, or κ, in the Cabibbo-allowed decay $D^+ \to K^-\pi^+\pi^+$ [3]. Further studies about κ are discussed in this proceeding [5].

In full Dalitz plot analyses, each possible resonance amplitude is represented by a Breit-Wigner function multiplied by angular distributions associated with the spin of the resonance. The various contributions are combined in a coherent sum with complex coefficients that are extracted from maximum likelihood fits to the data. The absolute value of the coefficients are related to the relative fraction of each contribution and the phases take into account the final state interaction (FSI) between the resonance and the third pion.

Due to the importance of this scalar meson in many areas of particle and nuclear physics, it is desirable to be able to confirm the amplitude's phase motion in a direct observation, without having to assume, a priori, the Breit-Wigner phase approximation for low-mass and broad resonances [6, 7, 8]. Recently, a method was proposed to extract the phase motion of a complex amplitude in three body heavy meson decays [2]. The phase variation of a complex amplitude can be directly revealed through the interference in the Dalitz-plot region where it crosses with a well established resonant state, represented by a Breit-Wigner.

Here we begin with a simple example, showing that the AD method can be applied to extract the resonant phase motion of the scalar amplitude due to the resonance $f_0(980)$, using the same $f_0(980)$ resonance in the crossing channel in the Dalitz plot of the decay $D_s^+ \to \pi^-\pi^+\pi^+$ using E791 data [9]. This example shows the ability of this method to extract the phase motion of an amplitude. Then we apply the AD method using the well known $f_2(1270)$ tensor meson in the crossing channel, as the base resonance, to extract the phase motion of the scalar low mass $\pi\pi$ amplitude in $D^+ \to \pi^-\pi^+\pi^+$, confirming the $\sigma(500)$ suggested by the E791 full Dalitz plot analysis [1].

2 Extracting $f_0(980)$ phase motion with the AD method.

From the original 2×10^{10} event data collected in 1991/92 by Fermilab experiment E791 from $500GeV/c\,\pi^- - nucleon$ interactions [10], and after reconstruction and selection criteria, we obtained the $\pi^-\pi^+\pi^+$ sample shown in Fig. 1. To study the resonant structure of these three-body decays we consider the 1686 events with invariant mass between 1.85 and 1.89 GeV/c^2, for the D^+ analysis and the 937 events with invariant mass between 1.95 and 1.99 GeV/c^2 for the D_s^+. Fig. 2(a) shows the Dalitz-plot for the $D_s^+ \to \pi^-\pi^+\pi^+$ selected events and Fig. 2(b) the Dalitz-plot for $D^+ \to \pi^-\pi^+\pi^+$ events. The two axes are the squared invariant-mass combinations for $\pi^-\pi^+$, and the plot is symmetrical with respect to the two identical pions.

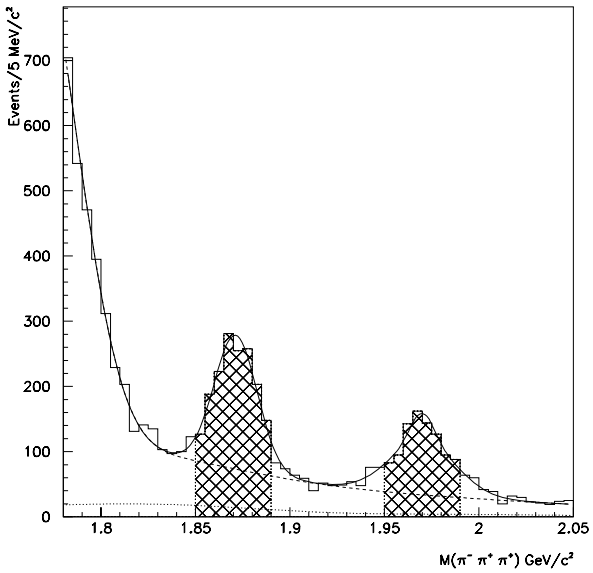

Figure 1. The $\pi^-\pi^+\pi^+$ invariant mass spectrum. The dashed line represents the total background. Events used for the Dalitz analyses are in the hatched areas.

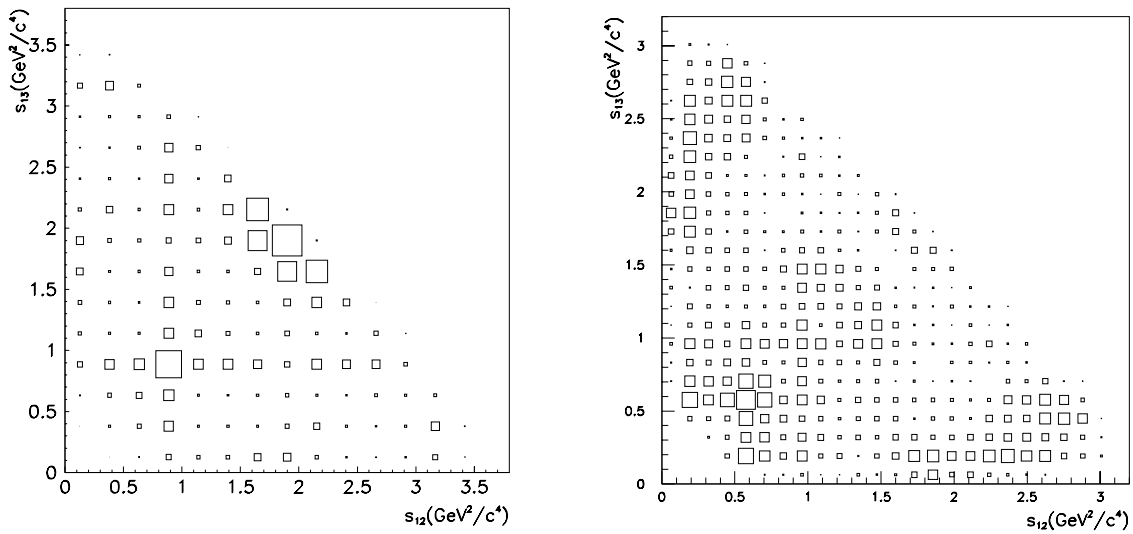

Figure 2. (a) The $D_s^+ \to \pi^-\pi^+\pi^+$ Dalitz plot and (b) the $D^+ \to \pi^-\pi^+\pi^+$ Dalitz plot. Since there are two identical pions, the plots are symmetrical.

We can see in Fig. 2(a) the scalar $f_0(980)$ in s_{12}, the square invariant mass, crossing the $f_0(980)$ in s_{13}, forming an interference region around $s_{13} = s_{12} = 0.95\text{GeV}^2$. The AD method uses the interference region, between two crossing resonances, to extract the phase motion of one of them, and Final State Interaction (FSI) phase, provided that the second is represented by a Breit-Wigner [2]. In fact we are using a *Bootstrap* approach; that is, using a well established resonance $f_0(980)$ in s_{12} to extract its phase motion in s_{13}. It is a nice and didactic example to show the ability of this method to extract the phase motion of an amplitude and the FSI phase within the E791 data sample.

The coherent amplitude to describe the crossing between a well known scalar resonance, represented by a Breit-Wigner in s_{12}, and a complex amplitude under study in s_{13} in a limited region of the phase space, where we can neglect any other contributions, is given by:

$$\mathcal{A}(s_{12}, s_{13}) = a_R \mathcal{BW}(s_{12}) + a_s/(p^*/\sqrt{s}_{13}) sin\delta(s_{13}) e^{i(\delta(s_{13})+\gamma)} \quad (1)$$

where $p^*/\sqrt{s}_{13}$ is a phase space factor to make this description compatible with $\pi\pi$ scattering, γ is the final state interaction (FSI) phase difference between the two amplitudes, a_R and a_s are respectively the real magnitudes of the resonance and the under-study complex amplitude. Finally $sin\delta(s_{13})e^{i\delta(s_{13})}$ represents the most general amplitude for a two-body hadronic interaction.

The Breit Wigner distribution is given by:

$$\mathcal{BW} = \frac{m_0\Gamma_0}{m_0^2 - s - im_0\Gamma(m)}$$

Taking the amplitude square of Equation 1 we get:

$$\begin{aligned} \mid \mathcal{A}(s_{12}, s_{13}) \mid^2 = a_R^2 \mid \mathcal{BW}_{f_0(980)}(s_{12}) \mid^2 + a_s^2/p^{*2}/s_{13} \;\; sin^2\delta(s_{13}) \\ + \frac{2a_R a_s m_0\Gamma_0 sin\delta(s_{13})/(p^*/\sqrt{s}_{13})}{(m_0^2 - s_{12})^2 + m_0^2\Gamma^2(s_{12})} \\ \times[(m_0^2 - s_{12})cos(\delta(s_{13}) + \gamma) + m_0\Gamma_0 sin(\delta(s_{13}) + \gamma)] \end{aligned} \quad (2)$$

Since the Breit-Wigner is approximately symmetrical around m_0 for the narrow $f_0(980)$ resonance as we can see in Fig. 3, we can divide our $f_0(980)$ mass distribution in two pieces, one for $m_0 + \epsilon$ and the other with $m_0 - \epsilon$. From Equation 2 and noticing that the non-crossing Breit-Wigner module square term will cancel we can write:

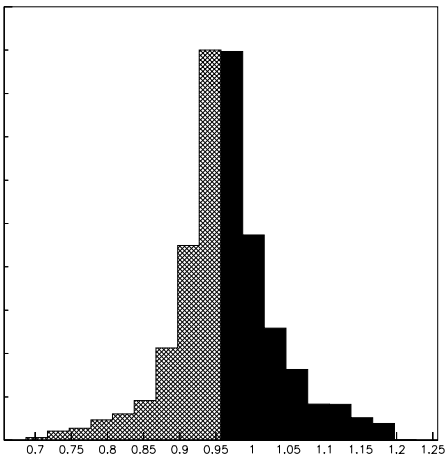

Figure 3. $f_0(980)$ s_{12} distribution, divided in $m_0 + \epsilon$ (black) and $m_0 - \epsilon$ (hatch)

$$\Delta \int \mathcal{A}^2 = \mid \mathcal{A}(m_0^2 + \epsilon, s_{13}) \mid^2 - \mid \mathcal{A}(m_0^2 - \epsilon, s_{13}) \mid^2 = \frac{-4a_R a_s m_0\Gamma_0/(p^*/\sqrt{s}_{13})\epsilon}{\epsilon^2 + m_0^2\Gamma_0^2}(sin(2\delta(s_{13}) + \gamma) - sin\gamma) \quad (3)$$

Only the real part of the interference term in Equation 2 remains.

To extract the phase motion of the scalar amplitude in s_{13} through the $f_0(980)$ in s_{12}, represented by a Breit-Wigner, we took the events in s_{12} between 0.7 and 1.2 GeV^2 and divided them into two bins, as presented in Fig. 3. The s_{13} distribution for the events of the s_{12} region integrated between 0.95 and 1.2 GeV^2, is shown in Fig. 4a and the same in Fig.4b for events integrated between 0.7 and 0.95 GeV^2.

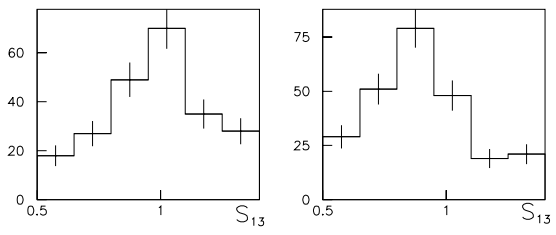

Figure 4. s_{13} distribution. a) For events $\int_{m_0^2}^{m_0^2+\epsilon} \mid \mathcal{A}(s_{12}, s_{13}) \mid^2 ds_{12}$. b) For events $\int_{m_0^2-\epsilon}^{m_0^2} \mid \mathcal{A}(s_{12}, s_{13}) \mid^2 ds_{12}$.

We can see that the peaks in these two plots are in different s_{13} positions. The subtraction of these distributions, corresponds to the integration of Equation 3, that we can write as:

$$\Delta \int \mathcal{A}^2 \sim -\mathcal{C}(sin(2\delta(s_{13}) + \gamma) - sin\gamma) \quad (4)$$

Where $\mathcal{C}$ is a constant factor coming from the constant and integrated factors of Equation 3, to be determined from data. The variation of the phase space in the integral was considered negligible for the $f_0(980)$ resonance. $\Delta \int \mathcal{A}^2$ directly reflects the behavior of $\delta(s_{13})$. A constant $\Delta \mid \mathcal{A} \mid^2$ would imply constant $\delta(s_{13})$. This would be the case for a non-resonant contribution. The same way a slow phase motion will produce a slowly varying $\Delta \mid \mathcal{A} \mid^2$ and a full resonance phase motion produces a clear signature in $\Delta \mid \mathcal{A} \mid^2$ with the presence of zero, maximum and minimum values.

The subtracted distribution, corresponding to Equation 4, is shown in Fig.5. There is a significant difference between the minimum (bin3) and maximum (bin4) of $\Delta \int \mathcal{A}^2$.

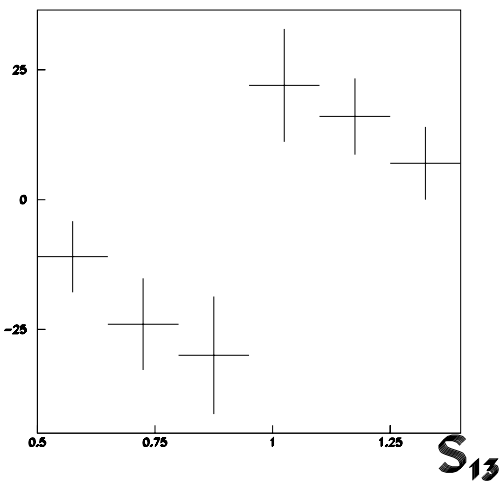

Figure 5. s_{13} distribution of $\Delta \int \mathcal{A}^2 ds_{12}$.

We can see in Equation 4 that the zeros occur when $\delta(s_{13})$ = 0^0, 180^0 or $\pi/2 - \gamma$. In Fig. 5 we can see a zero at s_{13} near 0.5GeV^2, another one at s_{13} = 0.95GeV^2 and a third zero near 1.4GeV^2. Assuming $\delta(s_{13})$ is an analytical function of s_{13}, Equation 4 allow us to set the two following conditions at the maximum and minimum values of $\Delta \int \mathcal{A}^2$ respectively:

$$\Delta \int \mathcal{A}^2_{max} \rightarrow sin(2\delta(s_{13}) + \gamma) = -1 \qquad (5)$$

$$\Delta \int \mathcal{A}^2_{min} \rightarrow sin(2\delta(s_{13}) + \gamma) = 1 \qquad (6)$$

With these two conditions we get $\mathcal{C}$ and γ, calculated from the maximum and minimum values of the $\Delta \int \mathcal{A}^2$ distribution in Fig. 5:

$$\mathcal{C} = (\Delta \int \mathcal{A}^2_{max} - \Delta \int \mathcal{A}^2_{min})/2 \qquad (7)$$

$$\gamma = sin^{-1}(\frac{\Delta \int \mathcal{A}^2_{max} + \Delta \int \mathcal{A}^2_{min}}{\Delta \int \mathcal{A}^2_{min} - \Delta \int \mathcal{A}^2_{max}}) \qquad (8)$$

From Fig. 5 and using the equations above, we measure $\gamma = -0.15 \pm 0.31$, that is compatible with zero, as should be since we are crossing the same resonances with, of course, the same final state interaction phase.

With the above conditions we solve Equation 4 for $\delta(s_{13})$:

$$\delta(s_{13}) = \frac{1}{2}(sin^{-1}(\frac{1}{\mathcal{C}}\Delta \mid \mathcal{A}(s_{13}) \mid^2 + sin(\gamma)) - \gamma) \qquad (9)$$

Assuming that $\delta(s_{13})$ is an increasing function of s_{13}, we can extract directly the $\delta(s_{13})$ value from each bin of Fig. 5. creating the $f_0(980)$ phase motion shown in Fig. 6. The errors in the plot were produced by generating statistically compatible experiments, allowing each bin of $\int_{m_0^2}^{m_0^2+\epsilon} \mid \mathcal{A}(s_{12}, s_{13}) \mid^2$ (Fig.4a) and $\int_{m_0^2-\epsilon}^{m_0^2} \mid \mathcal{A}(s_{12}, s_{13}) \mid^2$ (Fig.4b) to fluctuate randomly following a Poisson law. We then solve the problem for each "experiment". The error in each bin of $\delta(s_{13})$ will be the RMS of the distributions generated by the "experiments".

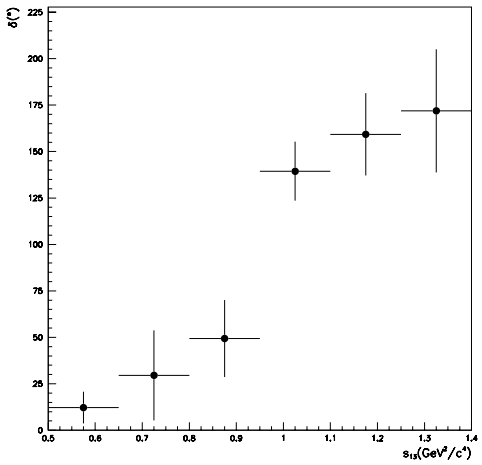

Figure 6. $\delta(s_{13})$ plot with the errors.

From Fig. 6 we can see what one could expect, that is the scalar amplitude near 970GeV with a phase motion of about 180^0 degrees. This example demonstrates the ability of AD method to extract the phase motion of an amplitude with E791 statistics.

3 Extracting the scalar low mass $\pi\pi$ amplitude phase motion with the AD method.

In the preceding section, we showed how to apply the AD method to extract the phase motion of an amplitude, from nonleptonic charm-meson three-body decay. Here we apply the same method to extract the phase motion of the scalar low-mass $\pi\pi$ amplitude in $D^+ \rightarrow \pi^-\pi^+\pi^+$ decay, where we previously found strong experimental evidence for the existence of a light and broad isoscalar resonance [1]. To start this analysis, we have to decide what is the best well-known resonance to be used for crossing the low mass amplitude under study. Taking a look at Fig. 2b we can see the signature of three resonances that in principle could be used, the $\rho(770)$, $f_0(980)$ and $f_2(1270)$. In fact, the E791 analysis of this Dalitz plot found a significant contribution from these three resonances in $D^+ \rightarrow \pi^-\pi^+\pi^+$ decay [1]. Since this D^+ decay is symmetric for the exchange of the π^+ meson, each resonance in s_{12} is present also in s_{13}. Then if we use $\rho(770)$ as the base resonance in s_{12}, we have also the presence of the $\rho(770)$ in same mass square distribution of the $\sigma(500)$ in s_{13}. The proximity of the $\rho(770)$ with the $\sigma(500)$, both broad resonances, creates an overlap between them such that we are not able to separate the phase motion of one from the other. We could use the $f_0(980)$ as a base

resonance, but again the presence of the $\rho(770)$ overlapping with the $\sigma(500)$ creates the same problem.

There remains only the tensor meson $f_2(1270)$ candidate at $m_0^2 = 1.61GeV^2$, which is placed where the $\rho(770)$ contribution reaches a minimum due the angular distribution in the middle of the Dalitz plot, as we can see from the $D^+ \to \rho(770)\pi^+$ decay Monte Carlo simulation shown in Fig. 7.

The amplitude for the crossing of the $f_2(1270)$ in s_{12} and the complex amplitude under study in s_{13} is given in the same way as in Equation 1:

$$\mathcal{A}(s_{12}, s_{13}) = a_R \;\; \mathcal{BW}_{f_2(1270)}(s_{12}) \;\; {}^{j=2}\mathcal{M}_{f_2(1270)}(s_{12}, s_{13}) + \\ + \;\; a_s/(p^*/\sqrt{s}_{13}) \;\; sin\delta(s_{13}) \;\; e^{i(\delta(s_{13})+\gamma)} \tag{10}$$

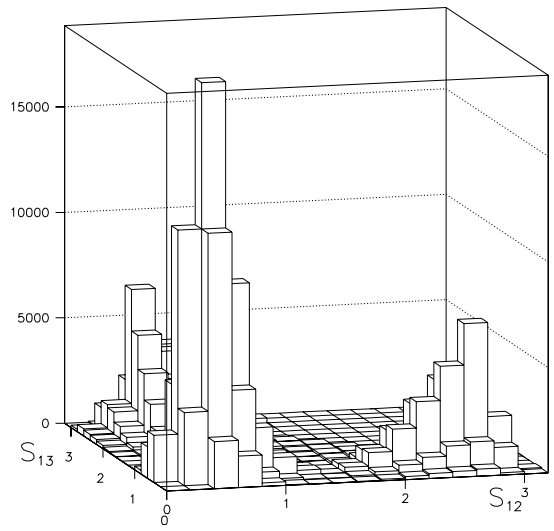

Figure 7. MC $\rho(770)$ distribution in $D^+ \to \pi^-\pi^+\pi^+$ decay. There is little contribution between 1.2 to 1.8GeV^2.

Where ${}^{j=2}\mathcal{M}_{f_2(1270)}(s_{12}, s_{13})$ is the angular function for the $f_2(1270)$ tensor resonance. The amplitude under study represents the scalar low mass $\pi\pi$ amplitude in a limited region of the phase space, where we can neglect the other amplitude contributions.

Both the width $\Gamma(s_{12})$ and the angular function ${}^{j=2}\mathcal{M}_{f_2(1270)}$ from this resonance produce asymmetries in s_{12} and consequently we can not use the nominal $f_2(1270)$ mass to divide our sample into two slices, as we did for the $f_0(980)$ example. So we performed a Monte Carlo study to determine the effective mass we must use. The s_{12} Monte Carlo projection of the $f_2(1270)$ in $D^+ \to \pi^-\pi^+\pi^+$ decay is shown in Fig. 8. We can see the asymmetry created around the nominal $f_2(1270)$ mass value due to $\Gamma(s_{12})$ and ${}^{j=2}\mathcal{M}_{f_2(1270)}$ contributions to the amplitude.

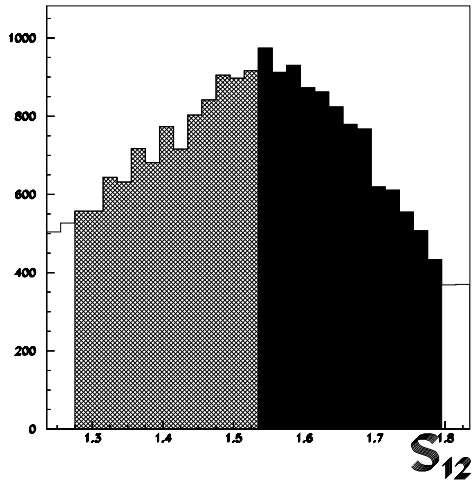

Figure 8. Monte Carlo $f_2(1270)$ s_{12} distribution, divided in $m_0+\epsilon$ (black) and $m_0 - \epsilon$ (hatch)

Here we require an effective mass squared (m_{eff}), such that the number of events integrated between m^2_{eff} and $m^2_{eff} + \epsilon$ is equal, by construction, to the number of events integrated between m^2_{eff} and $m^2_{eff} - \epsilon$. We choose, using the $f_2(1270)$ Monte Carlo distribution, a mass of $m^2_{eff} = 1.535GeV^2$, within $\pm 0.26GeV^2$ [1], in such way that we can write:

$$\int_{m^2_{eff}}^{m^2_{eff}+\epsilon} \mid \mathcal{BW}_{f_2(1270)}(s_{12})^{j=2}\mathcal{M}_{f_2(1270)} \mid^2 ds_{12} = \\ \int_{m^2_{eff}-\epsilon}^{m^2_{eff}} \mid \mathcal{BW}_{f_2(1270)}(s_{12})^{j=2}\mathcal{M}_{f_2(1270)} \mid^2 ds_{12} \tag{11}$$

The effective mass squared m_{eff} and the separation between $m^2_{eff} + \epsilon$ (black) and $m^2_{eff} - \epsilon$ (hatch) are shown in Fig. 8.

The ${}^{j=2}\mathcal{M}_{f_2(1270)}$ function in s_{13} is presented in Fig. 9[2]. The distribution between m^2_{eff} and $m^2_{eff} + \epsilon$ is shown in Fig. 9a, for events between m^2_{eff} and $m^2_{eff} - \epsilon$

[1] Within this mass region, the amount of $\rho(770)$ events was estimate to be around 5%

[2] Since we divided our data sample by this function, we represent this function in a histogram with the same binning of data.

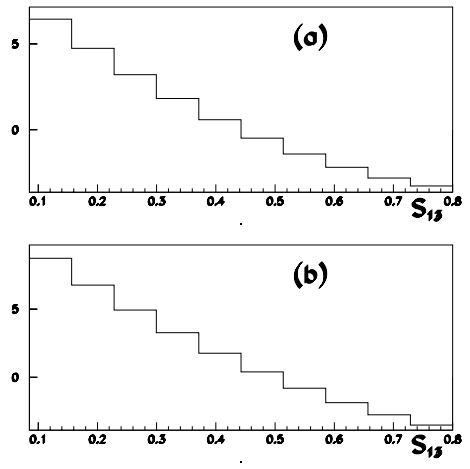

Figure 9. Fast MC ${}^{j=2}\mathcal{M}_{f_2(1270)}$ distribution in s_{13}. a) For events between m^2_{eff} and $m^2_{eff}+\epsilon$. b) For events between m^2_{eff} and $m^2_{eff}-\epsilon$.

in Fig. 9b. We can see that these two plots are slightly different. However we considered the approximation ${}^{j=2}\mathcal{M}^{+}_{f_2(1270)}(s_{13}) \sim {}^{j=2}\mathcal{M}^{-}_{f_2(1270)}(s_{13})$ and take an average function ${}^{j=2}\bar{\mathcal{M}}_{f_2(1270)}(s_{13})$. Another important effect, that we had to take into account, is the zero of this function at $s_{13} = 0.48GeV^2$. Below we discuss the consequences of that in the AD method.

With the above considerations about the $f_2(1270)$ in s_{12} and s_{13} we can write the integrated amplitude-square difference as:

$$\Delta\int\mathcal{A}^2 = \int_{m^2_{eff}}^{m^2_{eff}+\epsilon} \mid \mathcal{A}(s_{12},s_{13}) \mid^2 ds_{12} - \int_{m^2_{eff}-\epsilon}^{m^2_{eff}} \mid \mathcal{A}(s_{12},s_{13}) \mid^2 ds_{12}$$
$$\sim -\mathcal{C}(sin(2\delta(s_{13})+\gamma) - sin\gamma)\ {}^{j=2}\bar{\mathcal{M}}_{f_2(1270)}(s_{13})/(p^*/\sqrt{s}_{13}) \qquad (12)$$

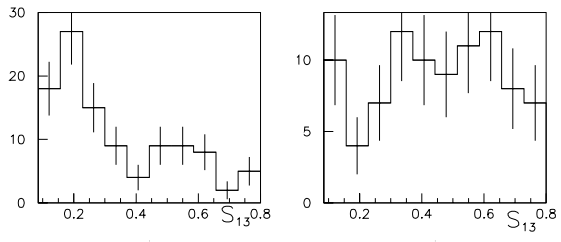

Figure 10. Events distributions in s_{13}, a) for events $\int_{m_0^2}^{m_0^2+\epsilon} \mid \mathcal{A}(s_{12},s_{13}) \mid^2 ds_{12}$, b) For events $\int_{m_0^2-\epsilon}^{m_0^2} \mid \mathcal{A}(s_{12},s_{13}) \mid^2 ds_{12}$.

This Equation is similar to Equation 4, with an extra angular function term ${}^{j=2}\bar{\mathcal{M}}_{f_2(1270)}(s_{13})$ [3].

The background and the acceptance are similar between m^2_{eff} and $m^2_{eff}+\epsilon$ and m^2_{eff} and $m^2_{eff}-\epsilon$. Since we are subtracting these two distributions, we do not take into account these effects in our analysis.

The $\int\mathcal{A}^2$ in s_{13}, for events integrated in s_{12} between $m^2_{eff} = 1.535GeV^2$ and $m^2_{eff}+\epsilon$ and m^2_{eff} and $m^2_{eff}-\epsilon$, with $\epsilon = 0.26GeV^2$ are presented in Fig. 10a and b respectively.

Subtracting these two histograms, in the same way we did for the $f_0(980)$ example, gives the $\Delta\int\mathcal{A}^2$ of the Equation 12. The result is shown in Fig. 11.

Here we can not extract directly the phase motion from Fig. 11, as we did for the $f_0(980)$ example using the conditions 5 and 6. We have to divide the $\Delta\int\mathcal{A}^2$ by $\bar{\mathcal{M}}$ (average of the distributions in Figs. 9a and b) and multiply by p', since phase space here is an important effect. By doing this the only s_{13} dependence of the right hand side of Equation 12 is in $\delta(s_{13})$. However, as we could see in Fig.9, there is a zero about 0.48GeV^2 in the angular function, which means a singularity around this value in $\Delta\int\mathcal{A}^2/\bar{\mathcal{M}}$. To avoid this singularity, we first produced a binning in such a way that the singularity is placed in the middle of one bin. In Fig. 12 we show the $\Delta\int\mathcal{A}^2$ by $\bar{\mathcal{M}}$ distribution. We can see that the 6th bin (around 0.48GeV^2), has a huge error, that corresponds to the bin of the singularity. Due to the singularity we decided not to use this region (bin 6) further in this analysis. The consequences of this choice are going to be taken care of in systematic error studies. In any case, the singularity

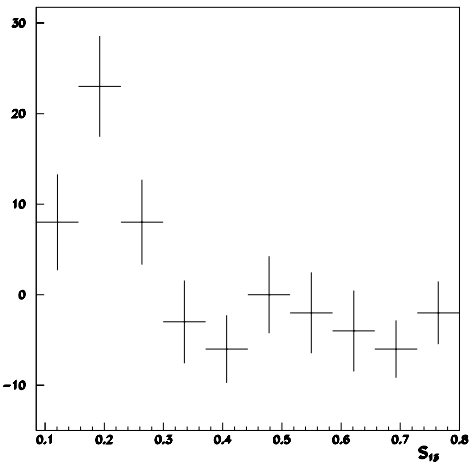

Figure 11. s_{13} distribution for $\Delta\int\mathcal{A}^2$.

[3] For short we shall use, from here on ${}^{j=2}\bar{\mathcal{M}}_{f_2(1270)}(s_{13}) = \bar{\mathcal{M}}$ and $p^*/\sqrt{s}_{13} = p'$.

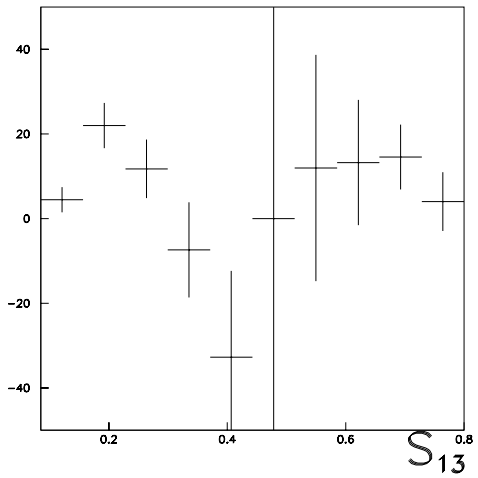

Figure 12. s_{13} distribution for $\Delta \int \mathcal{A}^2\ p'/\bar{\mathcal{M}}$.

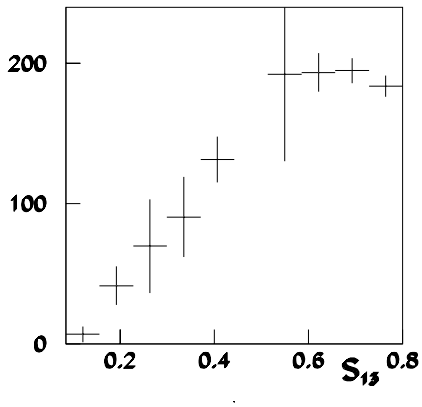

Figure 13. Phase motion $\delta(s_{13})$ distribution for the scalar low mass $\pi\pi$ amplitude, with the errors.

could only affect the position of the minimum of Fig. 12. It does not interfere with the general feature of starting at zero, having statistically significant maximum and minimum values, and coming back to zero, indicating a strong phase variation. Bins 2 and 5 are respectively the maximum and minimum value of $\Delta \int \mathcal{A}^2 p'/\bar{\mathcal{M}}$ of Fig. 12 where we use the Equation 5 and 6 conditions.

With the same assumptions used for the $f_0(980)$, that is $\delta(s_{13})$ is an analytical and increasing function of s_{13}, and using Equation 7, 8 and 9 (multiplied by p' and divided by $\bar{\mathcal{M}}$), we can extract γ and $\delta(s_{13})$ from Fig. 12. For the FSI phase we found $\gamma = 3.26 \pm 0.33$, that is somewhat bigger than found by the E791 full Dalitz-plot analysis [1] ($\gamma_{Dalitz} = 2.59 \pm 0.19$). The fact that we used the effective mass for the $f_2(1270)$ = 1.535 GeV^2 instead of the nominal mass is responsable for the shift observed in the relative phase. To verify this statement we generated 1000 samples of fast-MC, with only two amplitudes, $f_2(1270)$ and $\sigma(500)$. For both we used Briet-Wigner functions and the E791 parameters. We generated the phase difference of 2.59 rad, measured by the E791. For these 1000 samples, we measure γ using the method presented here. The result has a mean value of 3.07. We can say that the difference between the generated and measured γ value is a correction factor due to the use of an effective mass. Using this offset factor (2.59 - 3.07 = -0.48) we correct the measurement $\gamma = 3.26 \pm 0.33$ to $\gamma_{corr} = 2.78 \pm 0.33$. So the observed γ difference between Dalitz analysis and the γ_{corr} are in good agreement, with a difference below one standard deviation.

The $\delta(s_{13})$ was extracted bin by bin, with the same approach for the errors used in the $f_0(980)$ example, and we got the distribution shown in Fig. 13[4]. We can see a strong phase variation of about 180^0 around the mass for the $\sigma(500)$, showing a phase motion compatible with a resonance.

[4] In Fig.13 there is no the 6th bin because of the singularity we mentioned above.

4 Conclusions

We showed that the AD method can be applied to E791 data to extract the phase motion of the resonance $f_0(980)$ in the Dalitz plot of the decay $D_s^+ \to \pi^-\pi^+\pi^+$. This example demonstrates the ability of this method to extract the phase motion of a resonance amplitude.

Preliminary E791 results present a direct and model-independent approach, obtained with the AD method, and confirms our previous result of the evidence of an important contribution of the isoscalar $\sigma(500)$ meson in $D^+ \to \pi^-\pi^+\pi^+$ decay [1]. We use the well known $f_2(1270)$ tensor meson in the crossing channel, as the base resonance, to extract the phase motion of the low mass $\pi\pi$ scalar amplitude. We obtain a $\delta(s_{13})$ variation of about 180^0 consistent with a resonant $\sigma(500)$ contribution. We also obtain good agreement between the FSI γ_{corr} observed with AD method and the γ observed in the full Dalitz plot analysis.

References

[1] E791 Collaboration, E.M. Aitala *et al.*, Phys. Rev. Lett. **86**, 770 (2001).

[2] I. Bediaga and J. Miranda, Phys. Lett. B**550**, 135 (2002).

[3] E791 Collaboration, E.M. Aitala *et al.*, Phys. Rev. Lett. **89**, 121801 (2002).

[4] Particle Data Group, Hagiwara *et al.*, Phys. Rev. D **66**, 010001-1 (2002).

[5] Carla Göbel for E791 collaboration, this proceeding and hep-ex/0307003.

[6] Peter Minkowski and Wolfgang Ochs, hep-ph/0209225. To appear in the proceeding of QCD 2002 Euroconference, Montpellier 2-9 July 2002.

[7] J. A. Oller, hep-ph/0306294. To appear in the proceeding of Workshop on the CKM Unitarity Triangle, IPPP Durham, April 2003.

[8] A. D. Polosa, hep-ph/0306298. To appear in the proceeding of Workshop on the CKM Unitarity Triangle, IPPP Durham, April 2003.

[9] E791 Collaboration, E.M. Aitala *et al.*, Phys. Rev. Lett. **86**, 765 (2001).

[10] J.A. Appel, Ann. Rev. Nucl. Part. Sci. **42**, 367 (1992); D. Summers *et al.*, hep-ex/0009015; S. Amato *et al.*, Nucl. Instr. Meth. A **324**, 535 (1993); E.M. Aitala *et al.*, Eur. Phys. J. direct C**1**, 4 (1999); S. Bracker *et al.*, hep-ex/9511009; S. Bracker and S. Hansen, hep-ex/0210034; S. Hansen et al., IEEE Trans. Nucl. Sci. 34, 1003 (1987).